Journal of Metals, Materials and Minerals, Vol. 31, No. 2, pp. 84-88, 2021

Debinding behaviour and sintering temperature-dependent features of coloured zirconia fabricated by ceramic injection moulding

Wantanee BUGGAKUPTA[1,2], Thanakorn WASANAPIARNPONG[1,2], and Nutthita CHUANKRERKKUL[3,*]

[1] *Department of Materials Science, Faculty of Science, Chulalongkorn University, Phayathai Road, Bangkok, 10330, Thailand*
[2] *Center of Excellence on Petrochemical and Materials Technology, Chulalongkorn University, Phayathai Road, Bangkok, 10330, Thailand*
[3] *Metallurgy and Materials Science Research Institute, Chulalongkorn University, Phayathai Road, Bangkok, 10330, Thailand*

***Corresponding author e-mail:** nutthita.c@chula.ac.th

Received date:
24 January 2021
Revised date
18 April 2021
Accepted date:
23 April 2021

Keywords:
Coloured zirconia;
Ceramic injection moulding;
Sintering;
Water debinding;
Surface area to volume ratio

Abstract

Zirconia (ZrO_2) is one of ceramic materials that has very good mechanical and chemical properties suitable for biomedical applications as well as other industrial applications. ZrO_2 ceramics, in fact, has been used in orthodontic dentistry. Nowadays, ZrO_2 has been played its role in decorative and jewelry purposes, such as watchcases and artificial stones. Ceramic injection moulding (CIM), a near-net shape manufacturing process that can produce small, complex-shaped components and is suitable for large volume production, is one of the best powder fabrication methods. In this work, CIM was carried out in order to form the coloured-ZrO_2 specimens. Binders used in the feedstock preparation are composed mainly of polyethylene glycol (PEG) and polyvinyl butyral (PVB). A laboratory-scaled, plunger-typed injection moulding machine was used to fabricate the coloured-ZrO_2 components with various sizes and shapes. Debinding was carried out by water immersion and thermal debinding. Various sintering conditions were also performed. The specimens after sintering were subjected to be characterised and tested. The results showed that the binder removal rates using water related to geometry of the specimens, surface area and volume were taken into account. Sintering temperatures played important roles on properties, microstructure as well as the appearance and shades of the coloured-ZrO_2 fabricated by ceramic injection moulding.

1. Introduction

Ceramic injection moulding (CIM) technique is a category of powder injection moulding (PIM) which yields several advantages relative to other conventional ceramic forming processes. It has been reported that significant growth of global ceramic injection moulding market is anticipated by the year 2026 [1]. The CIM can overcome high precision, complex geometry, mass production, repeatability and waste management. CIM parts play their roles in many sectors including industrial machinery, healthcare, automotive, electrical and electronics. A feedstock contains a mixture of powder material with some binders, e.g. polyvinyl alcohol (PVA), polyvinyl butyral (PVB), polyethylene glycol (PEG), polymethyl methacrylate (PMMA) and paraffin wax, and other additives if required. Adapted from plastic injection moulding, either metal or ceramic powder is thoroughly blended with such polymer binders in a mixer before being fed into the mould or die cavity. When the blend is heated, a mixture becomes a paste which is soft and enables to flow and fill in the die. In the other word, injection ability is governed by several factors, for examples, nature of the paste (i.e. powder loading), binder types and amount used as well as injecting temperatures. After demoulding, the injected specimen is then undergone binder removal processes and sintering, respectively.

As far as the binders are concerned, binder removal methods of solvent debinding and thermal debinding are included. Therefore, the binders in PIM and CIM usually use as a binder mixture containing one which can be removed in a solvent while the other be removed during sintering. Normally the solvent-soluble binder is the key which always used in higher weight fraction compared to the others. Organic solvents, like hexane and n-heptane or even plain water, can possibly remove most of the majority binder [2-4] whereas the minority of the insoluble binder still exists to hold the powder compacts and promote handling ability before being burnt out while sintering.

Apart from alumina-based materials, zirconia (ZrO_2) injection moulding is recently of interests and comes into plays [5-8]. ZrO_2 has more and more routinely been used as structural, biomedical and other engineering ceramics. Due to specific outstanding features like high strength and toughness, it is also known as a ceramic steel. With superior physical, chemical and mechanical properties, ZrO_2 meets structural requirements and can be employed in various applications, e.g. cutting tools, dental implants, armors and gas sensors etc. Additionally, this material provides excellent resistance against corrosion, scratch and wear. The market of ZrO_2 for aesthetic applications has grown robustly in the last decades [1]. Recently, ZrO_2 applications as opaque accessories or decorative synthetic stones are also introduced, covering mobile phone backplates and smart wearable appearance parts, like watch cases and straps [9]. However,

it is not very simple to achieve the parts with such tiny, complex-shaped and high dimensional accuracy by means of machining or other conventional fabrication methods. Near-net shape CIM technique, therefore, is one of the most appropriate manufacturing processes that serves this purpose.

As for the binder systems used in a ZrO_2-based feedstock, they include water insoluble low density polyethylene (LDPE), high density polyethylene (HDPE) and paraffin wax. Zhao *et al.* [2] suggested the extraction of wax was fairly difficult in the stage of solvent debinding. This drawback could be solved by the partial replacement by LDPE while the replacement using HDPE could generate microcracks to the green parts when debinded in warm n-heptane. More gentle binder extraction could be achieved using milder solvents like water. A mixture of water-soluble binders, like PEG, with water-insoluble binder, such as PVB and PMMA, was reported elsewhere [9-13]. Hardmetal powders of WC-Co and WC-Ni could be successfully injected using a PEG/PMMA binder system [10,11]. Some studies focusing on alumina-matrix feedstocks with PEG/PVB binders suggested that water-soluble PEG removal rate depended on water temperature [12,14] as well as duration specimens immerged in water [12,13]. Therefore, the use of water-soluble binder may possibly apply to ZrO -based powder mixtures. As for the thermal processes, proper firing schedules are to be carefully designed: thermal debinding and sintering can be accomplished at the same time. During sintering, characteristics of the injected parts, e.g. density, pore content, strength, hardness, microstructural features and appearance, are substantially affected by firing temperatures. Higher temperatures generally result in higher density, coarser grains, improved flexural strength and hardness and can even alter colours.

Colours developed in ZrO_2 powder come from many sources, i.e. colouring oxides (e.g. Al_2O_3, NiO, CoO, Er_2O_3, Cr_2O_3, Fe_2O_3) or some industrial wastes [15]. The colours are diversified by many factors, including chemical composition, process history, initial particle size of the powder, agglomeration and sintering [9,17]. Luo *et al.* [15] explained that the as-sintered properties of yttria-stabilized ZrO_2 coloured by the addition of aluminium-chromium slag varied with sintering temperatures. Pink ZrO_2 derived from slag addition showed the changes in strength, microhardness, microstructure, fracture pattern as well as colour as a function of sintering temperatures. For dental purposes, high sintering temperature could intensify the yellow shade at 1450°C and became less chromatic at 1550°C [1], compared to the pre-stained blocks. Under atmospheric firing of N_2 and O_2 gas mixture, a variation in colours of the grey and yellow ZrO_2 between 700-1300°C was investigated and revealed that both colour alteration and translucency of 3YSZ dental ZrO_2 involved the level of oxygen vacancy, impurity and light scattering at grain boundary areas. [16,17].

This study focused on injection moulding of coloured ZrO_2 in two aspects: (1) the use of water-soluble PEG in coloured ZrO_2 powder and (2) the effects of sintering temperature on the coloured ZrO_2. Blue ZrO_2 powder was employed as a starting powder and well-mixed with a PEG/PVB binder system. The injected parts were undergone water leaching to remove PEG prior to being sintered at various temperatures. Water debinding ability as a function of specimen geometry was also mentioned. The influences of sintering temperatures on physical properties and colour alteration were observed and discussed.

2. Experimental procedures

A feedstock of a commercial 3 wt% yttria-stabilized ZrO_2 powder (TRZ-C-003, Daiichi Kigenso Kagaku Kogyo Co. Ltd., Japan) containing a slight amount of cobalt oxide (CoO) prepared by the manufacturer, was employed. The coloured ZrO_2 powder data sheet is as shown in Table 1. The density of this powder is 6.01 $g \cdot cm^{-3}$. Specific surface area and average particle size of the powder are 7.4 $m^2 \cdot g^{-1}$ and 0.56 μm, respectively, the morphology of which observed by a scanning electron microscope (SEM) is displayed in Figure 1. The blue ZrO_2 was evenly blended with two binders: PEG (average molecular weight of 1500) and PVB (average molecular weight of 80000). The weight ratio of PEG to PVB yielded 80:20. The powder loading of 38 vol% thoroughly mixed with the binder system was injected using a laboratory-scale plunger-type injection machine into a die cavity at the temperature of 160°C. Various geometries of the injected specimens including small disc-shaped, large disc-shaped, rectangular and irregular ones were introduced. Next, each specimen was carefully removed and naturally cooled down to ambient temperature (approximately 30°C) before debinding. Two steps of debinding were considered in this experiment: water debinding for PEG and thermal debinding for PVB. Firstly, the green specimens were immerged in still ambient water from 0.5, 1, 2, 4 up to 6 h to get the brown, PEG-eliminated, specimens. PEG removal rates by water were investigated from weight loss values before and after debinding. Secondly, the brown ones were heated up with the rate of 5°C·min^{-1} and soaked at 450°C for 2 h in air to completely get rid of PVB, followed by being sintered at 1350, 1450, 1500°C for 2 h using the same heating rate. Dimension of the specimens were then measured and calculated. Simplified surface area values were estimated using a grit method. The alteration in colour shades was quantitatively determined after CIELAB system by a colourimeter. Linear and volumetric changes, bulk density and water absorption after sintering were characterised and compared.

Table 1. Chemical composition of the blue partially-stabilized ZrO_2 powder (Material data form Daiichi Kigenso Kagaku Kogyo Co Ltd., Japan).

Oxides	Composition (wt%)
ZrO_2	94.55
Y_2O_3	3.56
Al_2O_3	1.89
H_2O	0.03
% Ignition loss (% L.O.I.)	0.41

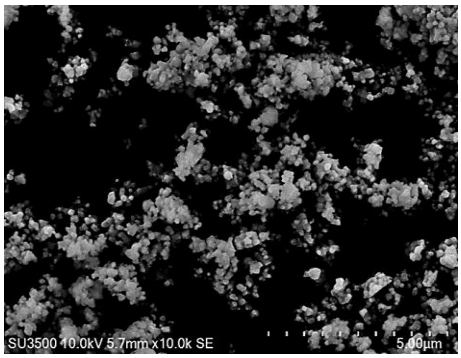

Figure 1. Morphological image of the blue partially-stabilized ZrO_2 powder.

3. Results and discussion

PEG binder removal using water is shown in Figure 2, illustrating the higher percentage of PEG binder was removed with longer immerged time. Total PEG removal in ceramic-matrix specimens with rectangular shape could be achieved within 6 h when immerged in water the temperature of which was kept above melting point of PEG [12,13]. This is because of the fact that the melting temperature of PEG (M.W. = 1500) is about 40°C to 43°C [12], so warm water could enhance diffusion of PEG so that PEG dissolved from the specimens relatively much quicker than ambient water. However, almost all PEG in the specimens could be gone within 24 h according to our further experiments. The difference in PEG removal values due to dimensional factor was also observed. Total PEG could be taken away in 6 h in rectangular and small disc specimens whereas those of irregular and large disc specimens were obviously slower. This may involve surface area and volume of the injected specimens.

Relationship between surface area and volume can be reported in the term of average surface area to volume ratio, as seen in Table 2. High surface area to volume ratio tends to be beneficial to binder removal, i.e. the higher ratio, the better PEG leaching [13]. Higher surface area to volume ratio represents the surface area that binder could travel towards solvent, in other words, the contact area that solvent could dissolve the binder from a specimen surface. Small volume reduces the distance binder travelling through the injected bodies from any sites in the specimen to the surface, regardless to a specimen contour. It was noticed that the large disc specimens owned the lowest surface area to volume ratio, 0.8, whereas those of small disc, rectangular and irregular specimens were about the same, falling between 1.20-1.55. From these values, it was expected to see the large disc specimens had the poorest PEG removal ability while the others had higher debinding ability. The rate PEG removal of the irregular shape was lower than that of the rectangular. This could be explained using average thickness and surface area information. Although the rectangular had greater volume compared with the irregular, it owned higher surface area with lower thickness, favoring water debinding. The rate PEG elimination of the rectangular shape, therefore, was superior to the irregular one.

The as-sintered properties including dimensional changes, bulk density, porosity and water absorption are reported in Table 3. Both linear and volumetric changes rose up with sintering temperatures. It was observed that dimensional changes, both linear and volumetric, at 1450°C and 1500°C were very close, indicating that the sintering temperature of 1450°C might be the optimum temperature for this coloured ZrO_2. As far as bulk density values were considered, the values strongly depend on sintering temperatures. Similarly, the densities obtained at 1500°C were very slightly different from those sintered at 1450°C, only a few percentage difference were conducted. Higher density values were derived with increasing temperatures. This brought about less pore content as well as water absorption. When the measured density values were relative to the theoretical density (TD) of coloured ZrO_2, 6.01 $g \cdot cm^{-3}$, it was pointed out that all specimens sintered at 1450°C met approximately 90%TD, as seen in Figure 3. Such %TD values with moderate strength seemed to be good enough for accessories, ornaments and decorative purposes. This might be a promising evidence to confirm that the optimum sintering temperature of this ZrO_2 powder was 1450°C unless different shades are required.

The variation in saturation of the blue colour was also presented. Figure 4 shows the shades of the specimens that gradually change from light blue to navy and eventually turn to indigo at 1500°C as a result of increasing sintering temperature. The colour quantitatively evaluated after CIELAB system is shown in Table 4, representing the lower L (lightness) values, or the darker blue, is obtained with increasing sintering temperatures. The saturation of blue was also more intense with increasing temperatures, regardless of the specimen shapes. In addition, higher sintering temperatures provided coarser grain sizes that make light less scatter and darken the colour in some extents [16]. Another explanation concerning colour darkening was solubility and ion exchange. Better solubility as well as exchange of Zr^{4+} and colouring metal ions are promoted by higher sintering temperatures [5,17,18]. However, a study concerning an ultrafine ZrO_2-Y_2O_3-CeO_2-Al_2O_3-CoO system [5] reported that the formation of $CoAl_2O_4$ and the reversible phase transformation of ZrO_2 solid solution as a function of heat treatment attributed to colour alteration. Unfortunately, the variations in grain size as well as phase composition according to the sintering temperatures upon these coloured ZrO_2 specimens are not yet reported herein and need to be done as our future work.

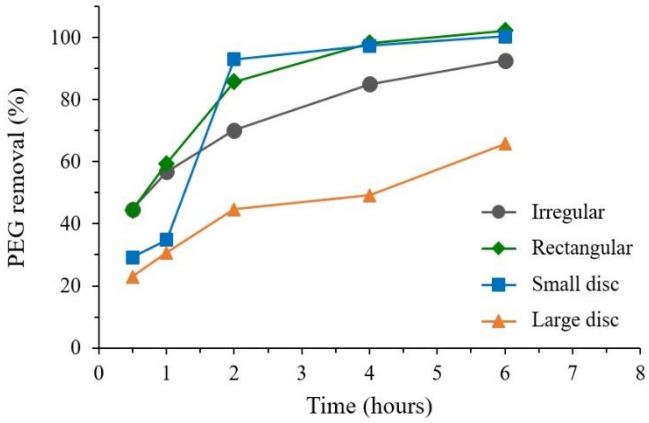

Figure 2. Degree of PEG removal from the injected specimens with various dimensions.

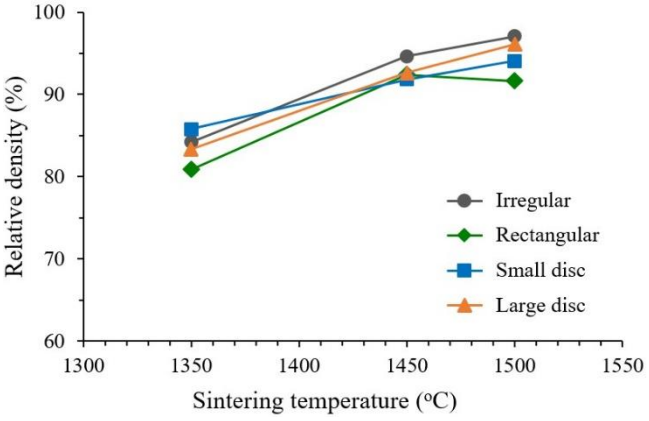

Figure 3. Relative density values of the ZrO_2 specimens sintered at various temperatures.

Table 2. Dimensional information of the as-injected ZrO_2 specimens with various geometries.

Sample shapes	Thickness (mm)	Surface area (mm^2)	Volume (mm^3)	Surface area to volume ratio (mm^{-1})
Irregular	2.00	364	240	1.52
Rectangular	1.37	920	600	1.53
Small disc	2.02	754	629	1.20
Large disc	3.21	1697	2121	0.80

Table 3. Physical properties of the as-sintered ZrO_2 specimens with various dimensions.

Sample shape	Sintering temperature (°C)	Linear shrinkage (%)	Volumetric shrinkage (%)	Bulk density ($g \cdot cm^{-3}$)	Water absorption (%)
Irregular	1350	22.35	50.19	5.06	2.66
	1450	27.40	59.52	5.69	0.86
	1500	29.30	61.76	5.83	0.54
Rectangular	1350	21.10	51.35	4.86	3.41
	1450	25.44	58.07	5.55	1.43
	1500	24.83	57.37	5.51	1.03
Small disc	1350	20.45	52.27	5.15	2.44
	1450	27.36	61.81	5.52	1.34
	1500	29.97	61.82	5.65	0.89
Large disc	1350	21.22	52.56	5.01	2.85
	1450	25.11	59.63	5.57	1.52
	1500	24.68	59.14	5.77	0.40

Table 4. Colour measurement (after CIELAB system) of the as-sintered ZrO_2 specimens.

Sintering temperature (°C)	Lightness L	Red-Green a*	Yellow –Blue b*
1350	63.44	3.53	-29.88
1450	45.82	7.68	-29.84
1500	44.19	6.74	-24.81

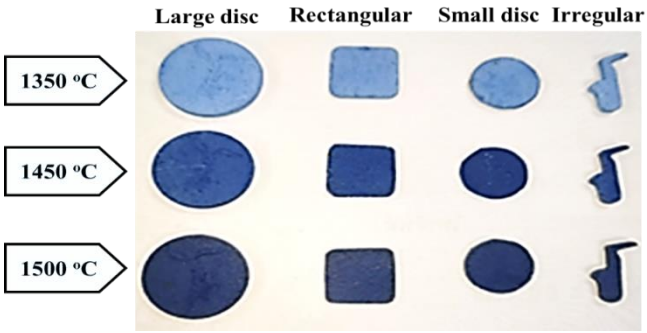

Figure 4. The colours of the as-sintered ZrO_2 specimens with various sintering temperatures.

4. Conclusions

A blue colour ZrO_2 powder feedstock could be successfully injected using a PEG-based binder system. The PEG binder more than 90% was removed by an ambient water within 6 h in all geometries. Higher sintering temperature led to deeper blue shade, along with higher density and shrinkage values. The relative density of 90%TD was achieved when sintered at 1450°C. Specimens sintered at 1450°C and 1500°C were very slightly different in the terms of density, shrinkage and colour shade, indicating that 1450°C might possibly be the optimum sintering temperature for accessory and decorative applications.

Acknowledgements

The authors are very grateful to the Metallurgy and Materials Science Research Institute and the Department of Materials Science, Faculty of Science, Chulalongkorn University. The authors would also like to thank Mr. Jasbadin Taweesubpermpoon, Mr. Peerakarn Mongkolsin and Miss Antika Boonruanganan for the preparation of specimens.

References

[1] T. Moritz, "Ceramic injection moulding: Developments in production technology, materials and application," *Powder Injection Moulding International*, vol. 14, pp. 55-81, 2020.

[2] M. Zhao, L. Qiao, J. Zheng, Y. Ying, J. Yu, W. Li, and H. Che, "Investigation of solvent debinding in injection moulding of zirconia ceramics using LDPE, HDPE and wax binders," *Ceramic International*, vol. 45, pp. 3894-3901, 2017.

[3] N. Saelee, N. Chuankrerkkul, and P. Wanakamol, "Microstructure and properties of zirconia-alumina composites fabricated via powder injection molding," *Journal of Metals, Materials, and Minerals*, vol. 31, pp. 73-80, 2021.

[4] Y. Gao, K. M. Huang, Z. K. Fan, and Z. P. Xie, "Injection molding of zircona ceramics using water-soluble binder," *Key Engineering Materials*, vol. 336-338, pp. 1017-1020, 2007.

[5] E. V. Dudnik, M. S. Glabay, A. V. Kotko, S. A. Korniy, and I. O. Marek, V. P. Red'Ko, and A.K. Ruban, "Effect of heat treatment on the physiochemical of ultrafine ZrO_2-Y_2O_3-CeO_2-Al_2O_3-CoO powders," *Power Metallurgy and Metal Ceramics*, vol. 59, pp. 359-367, 2020.

[6] G. De With, and P. N. M. Witbreuk, "Injection moulding of zirconia (Y-TZP) ceramics," Journal of the European Ceramic Society, vol. 12(5), pp. 343-351, 1993.

[7] A. P. Surzhikov, T. S Frangulyan, S. A. Ghyngazov, I. P. Vasil'ev, and A. V. Chernyavskii, "Sintering of zirconia ceramics by intense high-energy electron beam," Ceramics International, vol. 42(12), pp. 13888-13892, 2016.

[8] P. Khandelwal, and O. Sumant. (2019, 9 June, 2020). *Ceramic Injection Molding Market Forecast by Material and Industry Vertical: Global Opportunity Analysis and Industry Forecast, 2019–2026*. Available: https://www.alliedmarketresearch.com/ceramic-injection- molding-market

[9] S. Weng. (2018, 9 June, 2020). *The Overview of Colors Zirconia Ceramics*. Available: http://www.zirconiumworld.com/an-overview- of-colored- zirconia-ceramics/

[10] N. Chuankrerkkul, P. F. Messer, and H. A. Davies, "Application of polyethylene glycol and polymethyl methacrylate as a binder for powder injection moulding of hardmetals," *Chiang Mai Journal of Science*, vol. 35, pp. 188-195, 2008.

[11] N. Chuankrerkkul, Y. Boonyongmaneerat, K. Saengkiettiyut, P. Rattanawaleedirojn, and S. Saenapitak, "Injection moulding of tungsten carbide-nickel powders prepared by electroless deposition," *Key Engineering Materials*, vol. 545, pp. 148-152, 2013.

[12] W. Buggakupta, N. Chuankrerkkul, and J. Surawattana, "Effect of water temperature on water-soluble binder removal in ceramic materials fabricated by powder injection moulding," *Key Engineering Materials*, vol. 659, pp. 90-93, 2015.

[13] N. Chomsirikul, O. Khuanthong, P. Sooksaen, and N. Chuankrerkkul, "Influence of specimen dimension and temperature on debinding behavior of alumina feedstock," *Key Engineering Materials*, vol. 608, pp. 170-175, 2014.

[14] N. Chuankrerkkul, W. Buggakupta, and J. Surawattana, "Role of tungsten carbide reinforcement on alumina matrix composites fabricated by powder injection moulding," *Key Engineering Materials*, vol. 608, pp. 230-234, 2014.

[15] P. Luo, J. Zhang, X. Ran, and Y. Lui, "Effects of added aluminum chromium slag on the structure and mechanical properties of colored zirconia ceramics," *International Journal of Applied Ceramic Technology*, vol. 17, pp. 2659-2668, 2020.

[16] C. M. Chang, "Color variation in color-shade polycrystalline zirconia ceramics by the atmosphere controlled firing," *Journal of the Korean Ceramic Society*, vol. 55, pp. 116-125, 2018.

[17] E. Sani, D. Sciti, C. Capiani, and L. Silvestroni, "Colored zirconia with high absorbance and solar selectivity," Scripta Materialla, vol. 186, pp. 147,151, 2020.

[18] S. Ghyngazov, and S. Shevelev, "Effect of additives on sintering of zirconia ceramics," Journal of Thermal Analysis and Calorimetry, vol. 134, pp. 134, 2018.